Polymer 49 (2008) 3436–3443

Contents lists available at ScienceDirect

Polymer

journal homepage: www.elsevier.com/locate/polymer

Monodisperse temperature-responsive hollow polymer microspheres: Synthesis, characterization and biological application

Guoliang Li [a], Xiaoying Yang [b], Bin Wang [b], Junyou Wang [a], Xinlin Yang [a,*]

[a] Key Laboratory of Functional Polymer Materials, Ministry of Education, Institute of Polymer Chemistry, Nankai University, Tianjin 300071, China
[b] School of Pharmaceutical Sciences, Tianjin Medical University, Tianjin 300070, China

ARTICLE INFO

Article history:
Received 15 February 2008
Received in revised form 5 May 2008
Accepted 3 June 2008
Available online 7 June 2008

Keywords:
Temperature-responsive hollow microspheres
Distillation precipitation polymerization
Controlled drug release

ABSTRACT

Temperature-responsive hollow poly(*N*-isopropylacrylamide) (PNIPAAm) microspheres were prepared by a two-stage distillation precipitation polymerization to afford a core–shell microspheres with subsequent removal of poly(methacrylic acid) (PMAA) core. PMAA@PNIPAAm core–shell microspheres were synthesized by the second-stage polymerization of NIPAAm in the presence of PMAA as core with *N*,*N*′-methylenebisacrylamide as crosslinker in acetonitrile, in which the hydrogen-bonding interaction between the carboxylic acid group of PMAA core and the amide group of NIPAAm as well as MBAAm played a key role to form the core–shell microspheres. The hollow PNIPAAm microspheres with different thicknesses, which were controlled by the monomer loading level and the crosslinking degree, were developed after the removal of PMAA core. The loading and controlled-release behavior of the drug on the hollow PNIPAAm microspheres was investigated with doxorubicin hydrochloride. The core–shell and hollow microspheres were characterized with transmission electron microscopy, scanning electron microscopy, dynamic light scattering, static light scattering, X-ray photoelectron spectroscopy, elemental analysis, and FT-IR spectra.

1. Introduction

Polymer materials exhibit a range of super-molecular structures and functionalities, which potentially allow for chemical tailoring of the material properties for target-specific applications [1,2]. The main idea is to tailor the composition and function of polymer materials with precise control over the size and morphology at the submicrometer level. Core–shell particles are composite materials consisting of a core domain covered by a shell domain, which have found various applications in many areas, such as strengthening polymeric materials [3], and the stationary phases for chromatography or sensing materials [4]. One typical example is the formation of hollow nano-particles, which have found a wide-spread range of applications such as confined reaction vessels, drug carriers or protective shield for proteins, enzymes or DNA and for catalysis as well [5–9]. Significant progress has been made in the design and synthesis of hollow polymer particles by a variety of physical and chemical methods [10–14]. However, voided particles were prepared by emulsion polymerization through encapsulation of a hydrocarbon non-solvent, which is a process involving a number of convoluted, thermodynamic and kinetic factors [12]. Template-free techniques have been successfully utilized for the preparation of hollow polymer microspheres. Layer-by-layer assembly technique was suitable for polymer electrolytes with subsequent decomposition of the core [15–17]. Micelle formation of block copolymers to obtain hollow polymer microspheres involves the delicate design of the copolymer with UV crosslinking of the shell layer and the ozonolysis of the core [18]. Hollow polymer nano-spheres were afforded by surface-initiated atom-transform radical polymerization (ATRP) of styrene with subsequent UV treatment of the SiO_2-*g*-PS-*b*-PMMA core–shell hybrids for crosslinking and etching of the silica core in hydrofluoric acid [19]. On the one hand, the limited mechanical stability of micelles and vesicles prevents many potential applications (e.g. in drug delivery). On the other hand, high stability spheres with high degree of crosslinking result in low permeability, which prevents an effective loading of resultant capsules or releasing the encapsulated materials in a controlled way at the desired target. One promising strategy to solve these problems is to design "intelligent" hollow spheres with stimuli-responsive behavior. Many efforts have been made to produce smart micro-containers, in which the structure can be switched reversibly from closed state to an open state under different pH values [20], ionic strengths [21], and temperatures [13]. In this context, the preparation of temperature-responsive hollow polymer microspheres is particularly attractive, which is to fabricate the hollow spheres having characteristics controlled by the temperature.

* Corresponding author. Tel.: +86 22 23502023; fax: +86 22 23503510.
E-mail address: xlyang88@nankai.edu.cn (X. Yang).

0032-3861/$ – see front matter © 2008 Elsevier Ltd. All rights reserved.
doi:10.1016/j.polymer.2008.06.004

Monodispersity of the hollow polymer microspheres is very important to improve their performance in various applications. For instance, the polymer microspheres with uniform size are essential for drug delivery systems (DDS) because the distribution of the microspheres in the body and the interaction with biological cells are greatly influenced by the particle size [20]. Furthermore, if monodisperse microspheres are available, physical/chemical properties are uniform and the drug release kinetics can be manipulated, thereby making it easier to formulate more sophisticated intelligent DDS. However, few systematical investigations have been focused on the synthesis of monodisperse temperature-responsive hollow polymer microspheres and their controllable drug behavior under different temperatures.

Doxorubicin chloride (DXR) is a potent antibiotic for treatment of a variety of solid tumors and leukemias [22–25]. However, the cardiotoxicity of this drug is a serious drawback, which limits its direct administration and cumulative dosage [23]. The utilization of liposomes as drug delivery vehicles for administering DXR reduces the accumulation of the drug in the heart tissues by decreasing the concentration of free drug in circulation due to the stability of liposomes and their ability to retain the entrapped drug molecules (i.e., minimum leakage) [23,26,27].

In our previous work, monodisperse polymer microspheres with different functional groups on their surfaces [28–31] and hollow polymer microspheres with pyridyl groups on the interior surface [32] were prepared by distillation precipitation polymerization in neat acetonitrile with 2,2′-azobisisobutyronitrile (AIBN) as initiator. In the present work, monodisperse thermally responsive poly(*N*-isopropylacrylamide) (PNIPAAm) hollow microspheres with well-defined size and shell thickness were synthesized by a two-stage distillation precipitation polymerization in neat acetonitrile via varying *N*,*N*′-methylenebisacrylamide (MBAAm) crosslinking degree and monomer loading during the second-stage polymerization with subsequent removal of poly(methacrylic acid) (PMAA) core in water. The variation of the morphology and permeability for PNIPAAm hollow microspheres with increasing temperature was primarily investigated by dynamic light scattering (DLS).

2. Experimental section

2.1. Chemicals

N-Isopropylacrylamide (NIPAAm) was purchased from Acros Co. and recrystallized from hexane. *N*,*N*′-Methylenebisacrylamide (MBAAm, chemical grade, Tianjin Bodi Chemical Engineering Co.) was recrystallized from acetone. Methacrylic acid (MAA) was got from Tianjin Chemical Reagent II Co. and was purified by vacuum distillation. 2,2′-Azobisisobutyronitrile (AIBN, analytical grade, available from Chemical Factory of Nankai University) was recrystallized from methanol. Acetonitrile (analytical grade, Tianjin Chemical Reagents II Co.) was dried over 4 Å molecular sieves and purified by distillation. Doxorubicin hydrochloride (DXR) was provided by Beijing Huafeng United Technology Co. and used as-received. Dialysis chamber for the drug release was purchased from Beijing Dingguo Biotech Co. ($\Phi = 36$ mm), which had a molecular weight cut-off of 8000–15 000 g/mol. The other reagents were of analytical grade and used without any further purification.

2.2. Preparation of monodisperse PMAA@PNIPAAm core–shell microspheres by two-stage distillation precipitation polymerization

Monodisperse poly(methacrylic acid) (PMAA) microspheres were reported by distillation precipitation polymerization in neat acetonitrile with AIBN as initiator in the absence of any crosslinker [33], which was considered as the first-stage polymerization in the present work. A typical procedure for such polymerization was as follows: MAA (20 mL, 20 g, 0.23 mol) (as 2.5 vol% of the reaction medium), AIBN (0.4 g, 2.4 mmol, 2 wt% relative to the monomer) were dissolved in 800 mL of acetonitrile in a dried 1000 mL two-necked flask attached with a fractionating column, Liebig condenser, and a receiver. The flask was submerged in a heating mantle, and the reaction mixture was heated from ambient temperature till boiling state within 20 min, and then the solvent was distilled from the reaction system. The reaction mixture became milky white after boiling for 10 min. The reaction was ended after 400 mL of acetonitrile was distilled from the reaction system within 1.5 h. After the polymerization, the resultant PMAA microspheres were purified by repeating centrifugation, decanting, and resuspension in acetonitrile with ultrasonic bathing for three times.

Monodisperse poly(methacrylic acid)@poly(*N*-isopropylacrylamide) (PMAA@PNIPAAm) core–shell microspheres were synthesized in the presence of PMAA microspheres as seeds by the second-stage distillation precipitation polymerization of NIPAAm and MBAAm crosslinker with AIBN as initiator in acetonitrile. In a typical experiment, PMAA (0.20 g), NIPAAm (0.4 g, 3.54 mmol), MBAAm crosslinker (0.06 g, 0.38 mmol, 10 mol% corresponding to the monomers of NIPAAm and MBAAm) and AIBN (0.01 g, 0.06 mmol, 2 wt% relative to the monomers) initiator were dispersed in 80 mL of acetonitrile at room temperature in a 100-mL two-necked flask equipped with a fractionating column, Liebig condenser, and a receiver. The flask was submerged in a heating mantle and the second-stage polymerization mixture was heated from ambient temperature till boiling state within 30 min. The polymerization was continued further under boiling state for 20 min when the solvent was distilled from the reaction system. The reaction was ended after 40 mL of acetonitrile was distilled off the reaction mixture within 2 h. After the reaction, the resultant PMAA@PNIPAAm core–shell microspheres were purified by three cycles of ultracentrifugation, decanting and redispersion in acetonitrile with ultrasonic irradiation.

The PMAA@PNIPAAm core–shell microspheres with different shell thicknesses and crosslinking degrees of PNIPAAm shell layer were conveniently prepared by the second-stage distillation precipitation polymerization via altering the amount of NIPAAm and MBAAm crosslinker, while the amount of AIBN initiator was maintained at 2 wt% relative to the total monomers. The crosslinking degree was referred as mol% of MBAAm crosslinker relative to the total monomers of MBAAm and NIPAAm. The treatment of these core–shell particles was the same as that for the typical process.

2.3. Synthesis of hollow PNIPAAm microspheres

Monodisperse PMAA@PNIPAAm core–shell microspheres with various shell thicknesses and crosslinking degrees were dialyzed in de-ionized water at room temperature for selective dissolution of PMAA cores. The dialysis process to obtain hollow PNIPAAm microspheres lasted two weeks for complete removal of PMAA core. The resultant PNIPAAm hollow microspheres were dried in a vacuum oven at room temperature till constant weight.

2.4. Loading of DXR onto PNIPAAm hollow microspheres

Doxorubicin hydrochloride (DXR, 0.20 mg) was dissolved in 10 mL of 0.9 wt% NaCl solution and then 8.0 mg of PNIPAAm hollow microspheres was suspended in this solution. The loading of the drug took place in the suspension on an SHA-B shaker with gentle agitation by rolling the bottles in a horizontal position to approximately 40 rpm for three days. The unloaded DXR molecules were removed by ultracentrifugation. The loading capacity of DXR on PNIPAAm hollow microspheres was determined by ultraviolet

spectrum (UV), which was calculated by the difference of DXR concentration between the original DXR solution and the supernatant after loading. In this process, the supernatant after ultracentrifugation in the presence of PNIPAAm hollow microspheres without DXR was used as a blank sample for determination, in which DXR concentration was calibrated from a standard curve of DXR/NaCl (0.9 wt%) solution.

2.5. Release of DXR from PNIPAAm hollow microspheres

The drug-loaded PNIPAAm hollow microspheres (8 mg) were dispersed in 4 mL of 0.9 wt% NaCl soution and the dispersion was divided into two equal aliquots. The drug-loaded hollow polymer samples used for the release experiments were placed into the dialysis chambers, which were dialyzed in 80 mL of 0.9 wt% NaCl solution at 20 and 40 °C, respectively. The drug release was assumed to start as soon as the dialysis chambers were placed into the reservoir. The release reservoir was kept under constant stirring, and at various time points, one of the dialysis chambers was taken out for characterization. The concentration of DXR released from PNIPAAm hollow microspheres into distilled water was quantified using UV spectroscopy.

2.6. Characterization

The morphology of the resultant polymer microspheres was determined by transmission electron microscopy (TEM) using a Technai G^2 20-S-TWIN microscope. Samples for TEM characterization were dispersed in solvent and a drop of the dispersion was spread onto the surface of a copper grid coated with a carbon membrane and then dried in vacuum at room temperature for characterization.

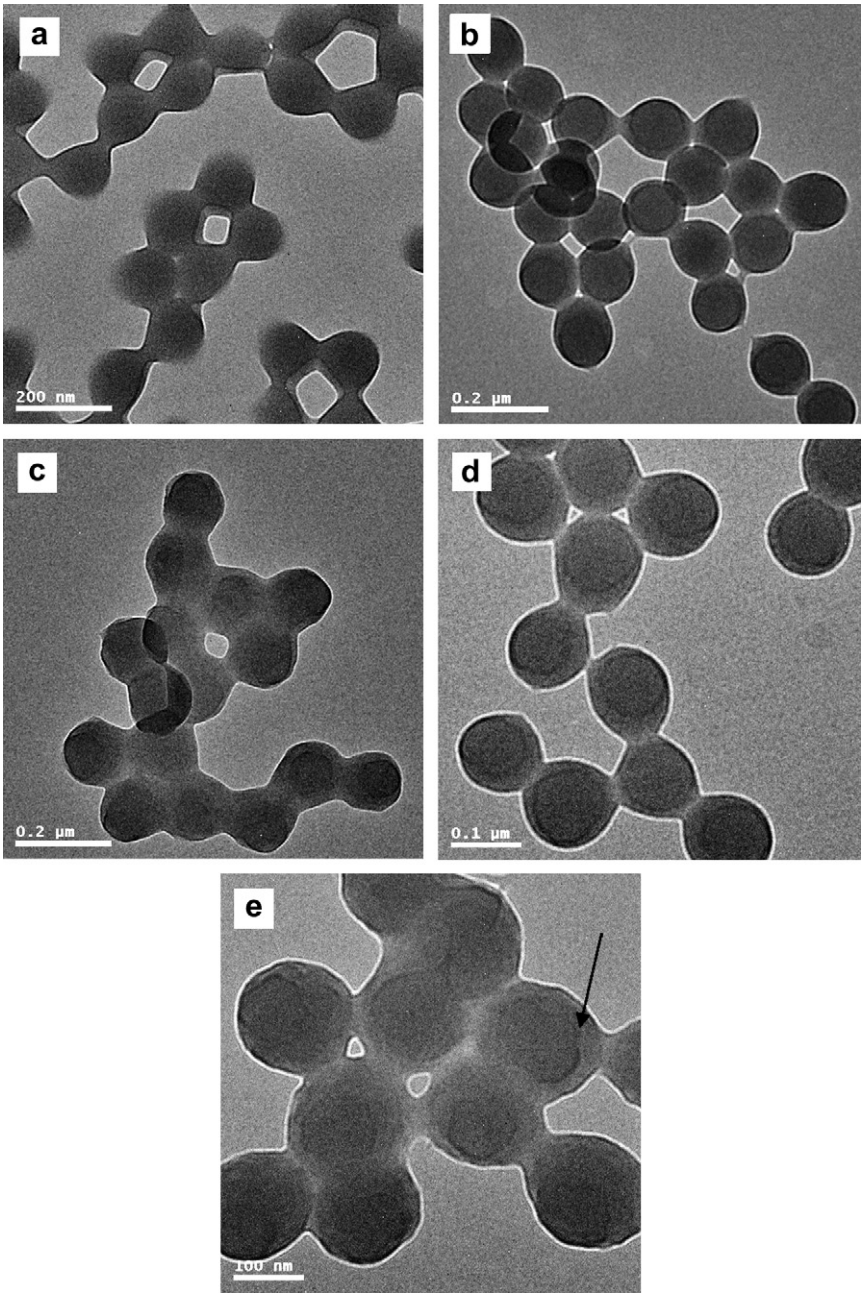

Fig. 1. TEM micrographs of PMAA@PNIPAAm core–shell microspheres with different thicknesses of the shell layer controlled by NIPAAm monomer and MBAAm crosslinker amount: (a) PMAA core; (b) $CS_{10\text{-}1}$; (c) $CS_{10\text{-}3}$; (d) $CS_{5\text{-}2}$; (e) $CS_{20\text{-}2}$.

Table 1
Reaction conditions, size and size distribution of PMAA@PNIPAAm core–shell microspheres

Entry	Crosslinking degree (mol%)	NIPAM/PMAA (w/w)	D_n (nm)	D_w (nm)	U	Shell thickness[a] (nm)
PMAA	–	–	121	122	1.006	_
CS_{10-1}	10	1	120	121	1.011	_
CS_{10-2}	10	2	129	130	1.011	4
CS_{10-3}	10	3	132	133	1.006	6
CS_{10-4}	10	4	138	139	1.006	9
CS_{5-2}	5	2	115	117	1.012	_
CS_{15-2}	15	2	155	156	1.006	17
CS_{20-2}	20	2	177	178	1.010	28

[a] The thickness of the shell layer calculated as the half of the difference in diameters between PMAA core and PMAA@PNIPAAm core–shell microspheres.

Scanning electron microscopy (SEM) was obtained using a HITACHI S-3500N microscope. The samples for SEM determination were prepared by dispersing polymer particles in a solvent and then placing one drop of the dispersion on a piece of glass slide onto an electron microscope stub with double-sided adhering tape. The samples were dried under vacuum for 24 h at room temperature and sputter-coated with Au nano-particles.

All the size and size distribution reflect the averages of about 100 particles, which are calculated according to the following formula:

$$U = D_w/D_n\, D_n = \sum_{i=1}^{k} n_i D_i / \sum_{i=1}^{k} n_i\, D_w = \sum_{i=1}^{k} n_i D_i^4 / \sum_{i=1}^{k} n_i D_i^3$$

where U is the polydispersity index, D_n is the number-average diameter, D_w is the weight-average diameter, D_i is the particle diameter of the determined microparticles.

Fourier transform infrared spectra were determined on a Bio-Rad FTS 135 FT-IR spectrometer over potassium bromide pellet and the diffuse reflectance spectra were scanned over the range of 4000–400 cm^{-1}.

UV–vis absorption spectra were measured on a JASCO V-570 UV–Vis spectrometer with a laser source of wavelength at 234 nm as an excitation source for the determination of the concentration of DXR.

X-ray photoelectron spectroscopic (XPS) analysis was carried out with a PHI 5300 XPS surface analysis system (Physical Electronics, Eden Prairie, MN, US) using an Mg Kα X-ray source operating at 250 W and 13 kV ($h\nu = 1253.6$ eV). The electron binding energy of C_{1s} (284.6 eV) was used as the internal standard.

Elemental analysis (EA) was performed on a Perkin–Elmer-2400 to determine the nitrogen, carbon and hydrogen contents of the resultant polymer particles.

Dynamic light scattering (DLS) and static light scattering (SLS) measurements were performed in a laser scattering spectrometer (BI-200 SM) equipped with a digital correlation (BI-10000 AT) at 636 nm. All the samples were prepared from the suspension with concentration of about 1 mg/mL after ultrasonic irradiation and were then measured at 25 and 50 °C, respectively. The hydrodynamic diameter (D_h) and the polydispersity index of the size distribution were obtained by a cumulant analysis.

3. Results and discussion

Distillation precipitation polymerization has been proven to be a useful and facile technique for the synthesis of monodisperse polymer microspheres with different functional groups and the functional core–shell microspheres [28–33]. The TEM micrograph of PMAA microspheres by distillation precipitation polymerization is shown in Fig. 1a, which indicated that the polymer microspheres had spherical shape and smooth surface with an average size of 121 nm, a polydispersity index (U) of 1.006 as summarized in Table 1.

3.1. Preparation of PMAA@PNIPAAm core–shell microspheres

In the present work, the PMAA microsphere without any crosslinker would be used as the template for the synthesis of core–shell microsphere. The results have demonstrated that acetonitrile was a suitable medium for the efficient hydrogen-bonding interaction between carboxylic acid group and pyridyl group [34] as well as the synergic hydrogen-bonding interaction between the carboxylic acid and amide group [31] acting as a driving force for the construction of raspberry-like polymer composites. Here, the synergic hydrogen-bonding interaction between the carboxylic acid group on the surface of PMAA core and amide group of NIPAAm as well as MBAAm crosslinker played a key role to promote the formation of monodisperse PMAA@PNIPAAm core–shell microspheres as illustrated in Scheme 1.

A series of experiments were initially designed to investigate the monomer concentration on the preparation of the PNIPAAm shell with the crosslinking degree of 10 mol% MBAAm, in which the NIPAAm concentration was varied from 1/1 to 4/1 (relative to the mass of PMAA core) for the second-stage polymerization. All other components including the initiator level at 2 wt% (corresponding to

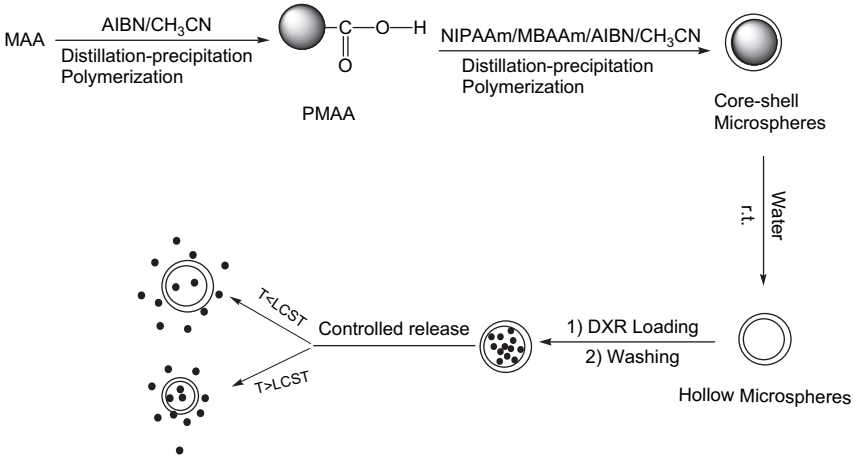

Scheme 1. Preparation of PMAA@PNIPAAm hollow microspheres and their controlled-release behavior as drug carrier.

the whole monomers) and the distillation rate of acetonitrile were held constant during the second-stage polymerization. The TEM micrographs of the resultant PMAA@PNIPAAm core–shell microspheres with different NIPAAm concentrations for the shell layer ($CS_{10\text{-}1}$ and $CS_{10\text{-}3}$ as samples) are shown in Fig. 1b and c, which indicated that the core–shell microspheres had spherical shape with smooth surface. All of the PMAA@PNIPAAm core–shell microspheres occurred as multiplet and with some coagulum observed in TEM images, which may be due to the strong interparticle hydrogen-bonding interaction and soft surface of the polymer microspheres with low crosslinking degree.

The reaction conditions, size and size distribution of the final PMAA@PNIPAAm core–shell microspheres with various NIPAAm loadings for the synthesis of the shell layer are summarized in Table 1. The average diameters were considerably increased from 120 to 138 nm with increasing NIPAAm feed from 1/1 to 4/1 (mass ratio to PMAA core) for the second-stage polymerization, and the corresponding shell thickness of PNIPAAm layer increased to 9 nm, while the core–shell polymer microspheres maintained monodisperse with polydispersity index below 1.011. The diameter of PMAA@PNIPAAm core–shell microspheres with NIPAAm loading of 1/1 (mass ratio to PMAA core) for the second-stage polymerization was 120 nm with monodispersity index of 1.011, which was due to the formation of the crosslinked dense shell after the second-stage polymerization to shrink the whole diameter of the core–shell polymer microspheres. When NIPAAm feed in the second-stage polymerization was increased to higher than 2/1, the size of the final PMAA@PNIPAAm core–shell microspheres was considerably larger than that of PMAA core (121 nm) and the maximum diameter of 138 nm with polydispersity index of 1.006 was obtained at NIPAAm feed of 4/1 (mass ratio to PMAA core).

To understand the effect of MBAAm crosslinker on the formation of PNIPAAm shell layer, the crosslinking degree was varied from 5 to 20 mol% during the second-stage polymerization, while the NIPAAm feed was kept at 2/1. The TEM images of the prepared PMAA@PNIPAAm core–shell particles with different MBAAm crosslinking degrees ($CS_{5\text{-}2}$ and $CS_{20\text{-}2}$ as samples) are shown in Fig. 1d and e. The results indicated that the resultant polymer microspheres had spherical shape with smooth surface. The TEM micrographs confirmed the core–shell structure of the final polymer microspheres, especially in the case of higher crosslinking degree (20 mol%) as identified by an arrow in Fig. 1e.

The effect of MBAAm as a crosslinker on the formation of the PMAA@PNIPAAm core–shell structure is listed in Table 1. The size of the core–shell microsphere was increased significantly from 115 nm at crosslinking of 5 mol% ($CS_{5\text{-}2}$, Fig. 1d) to 177 nm at MBAAm of 20 mol% ($CS_{20\text{-}2}$, Fig. 1e), and the corresponding shell thickness of PNIPAAm was considerably enhanced from 4 nm to 28 nm, while the polydispersity index was maintained at monodisperse below 1.012. The size of the final core–shell microspheres was generally determined by the nuclei and the conversion of the monomers in the system. The absence of the second-initiated small particles in the resultant system indicated that the number of nuclei was a constant value during the second-stage polymerization, which was controlled by the number of PMAA seeds used. Such results demonstrated that the capture ability of the PMAA core with the aid of the synergic hydrogen-bonding interaction as shown in Scheme 1 was enough to result in monodisperse PMAA@PNIPAAm core–shell microspheres during the second-stage polymerization without formation of the second-initiated particles.

The seed polymerization of NIPAAm leading to PMAA@PNIPAAm core–shell microspheres was studied by FT-IR spectra and is shown in Fig. 2. In addition to the peak at 1699 cm^{-1} corresponding to the characteristic stretching vibration of the carbonyl group in PMAA segment, the FT-IR spectrum of PMAA@PNIPAAm core–shell particles in Fig. 2b had a new strong peak at 1534 cm^{-1} assigning to

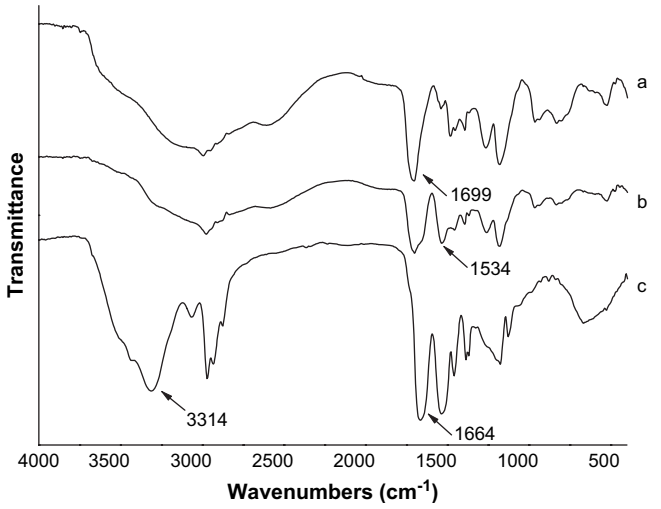

Fig. 2. FT-IR spectra of: (a) PMAA core; (b) PMAA@PNIPAAm core–shell microspheres; (c) PNIPAAm hollow microspheres.

the vibration of the second-amide group of NIPAAm as well as MBAAm segments. To prove the core–shell structure further, the surface components of PMAA core and PMAA@PNIPAAm microspheres with crosslinking degree of 15% as a sample were determined by XPS spectra and are shown in Fig. 3, in which the electronic binding energy of C_{1s} (284.6 eV) was used as the internal standard. The XPS spectrum of PMAA@PNIPAAm microspheres had

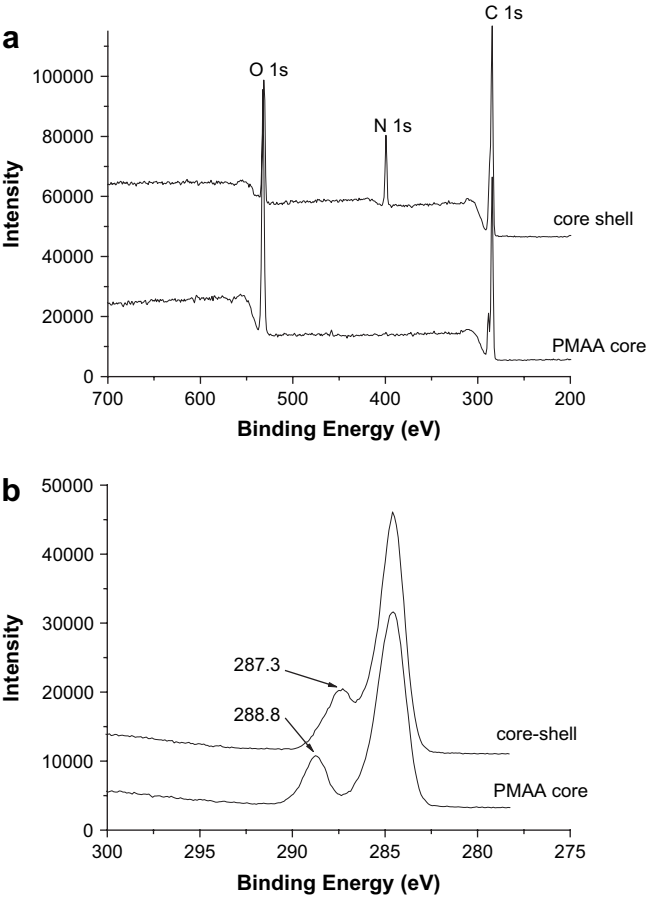

Fig. 3. XPS spectra of PMAA core and PMAA@PNIPAAm core–shell microspheres: (a) binding energy of O_{1s}, N_{1s}, and C_{1s}; (b) curve fitting of the C_{1s} photoelectron peak.

Table 2
The elemental analysis of the polymer particles[a]

Entry	N (%)
PMAA	0.45
PMAA@PNIPAAm	3.67
Hollow PNIPAAm	9.28
Eluted core	2.58

[a] PMAA@PNIPAAm and hollow PNIPAAm microspheres with 15 mol% crosslinking degree as a sample.

the peaks at 531.4, 399.7, and 288.0 eV (Fig. 3a) ascribing to the binding energy of O_{1s}, N_{1s}, and C_{1s}, respectively. While for the XPS spectrum of PMAA core, only the peaks at 531.4 and 288 eV corresponding to the binding energy of O_{1s} and C_{1s} were observed in the absence of peak at 399.7 eV for N_{1s}. Furthermore, the XPS results in Fig. 3b indicated that part of the peak at 288.8 eV was shifted to 287.3 eV. The former can be attributed to the C core level of the carbonyl group of the carboxylic acid component in PMAA core and the latter was assigned to the C core level of carbonyl group of amide component in PMAA@PNIPAAm. These PMAA@PNIPAAm microspheres with core–shell structure were also confirmed by the elemental analysis listed in Table 2. The N content of PMAA core was only 0.45% (the residual part of AIBN initiator) and that of PMAA@PNIPAAm core–shell microsphere was considerably enhanced to 3.67%.

All the results from TEM, FT-IR and XPS characterization confirmed the successful formation of the core–shell structure during the second-stage polymerization of MBAAm crosslinker and NIPAAm. Our approach via using hydrogen-bonding interaction to form core–shell structure without any additive has the advantage that it is much easier and simpler than some complex modification process of template, such as attaching an initiator onto the silica surface to achieve a controlled living polymerization, modification of silica template with MPS and polystyrene particles with concentrated sulfuric acid.

3.2. Monodispersed PNIPAAm hollow microspheres

PMAA cores of the resultant PMAA@PNIPAAm core–shell microspheres were selectively removed by the dissolution in water to afford PNIPAAm hollow microspheres. The typical TEM and SEM micrographs of PNIPAAm hollow microspheres with NIPAAm feed of 2/1 and MBAAm crosslinking degree of 20 mol% are shown in Fig. 4a and b, in which convincing hollow-sphere structures were observed with the presence of circular rings of sectioned spheres and a cavity in the interior. The complete disappearance of 1699 cm^{-1} corresponding to the carbonyl group of carboxylic acid unit of PMAA segment in FT-IR spectrum of PNIPAAm hollow microspheres as shown in Fig. 2c, the presence of the strong peaks at 3314 cm^{-1} assigning to the characteristic peaks of vibration for N–H group and the strong peak at 1664 cm^{-1} due to the stretching vibration of carbonyl group of amide in PMBAAm as well as PNIPAAm segment proved the successful removal of the PMAA core by dissolution to result in PNIPAAm hollow structure. The driving force for such removal to afford the PNIPAAm hollow microspheres was based on the solubility of the non-crosslinked polymer core in water at room temperature, which was much mild and environmentally friendly without utilization of highly corrosive reagent, such as hydrofluoric acid (HF) in the case of silica as sacrificial core [35].

The elemental analysis was used to determine the composition of PMAA core, PMAA@PNIPAAm core–shell microspheres, hollow PNIPAAm microspheres and the eluted core for the formation of hollow PNIPAAm microsphere (with crosslinking degree of 15% as a sample) and is summarized in Table 2. The nitrogen content of hollow PNIPAAm microspheres was significantly increased from 3.67% of PMAA@PNIPAAm core–shell microspheres to 9.28%, which was near to the nitrogen content of neat PNIPAAm (12.3%), which indicated that the shell of hollow polymer microspheres was mainly composed of PNIPAAm. All these results proved further the preparation of PMAA@PNIPAAm core–shell microspheres by two-stage distillation precipitation polymerization and the subsequent development of hollow PNIPAAm microsphere after the selective removal of the non-crosslinked core.

The hydrodynamic diameters from DLS characterization and the corresponding polydispersity index of the resultant PNIPAAm hollow microspheres are summarized in Table 3. The hydrodynamic size of the hollow microspheres, which were developed from the PMAA@PNIPAAm core–shell microspheres, increased drastically from 315 nm at NIPAAm feed of 1/1 to 483 nm at NIPAAm feed of 4/1 with crosslinking degree of 10 mol%. The polydispersity index of the hydrodynamic diameters was narrow in the range of 1.136–1.198, which was a little broader than that from TEM characterization. The much larger hydrodynamic diameters from DLS in water than those from TEM observation proved the hydrophilic property of the resultant PNIPAAm hollow microspheres, as the former ones were determined as in a swollen state. The typical

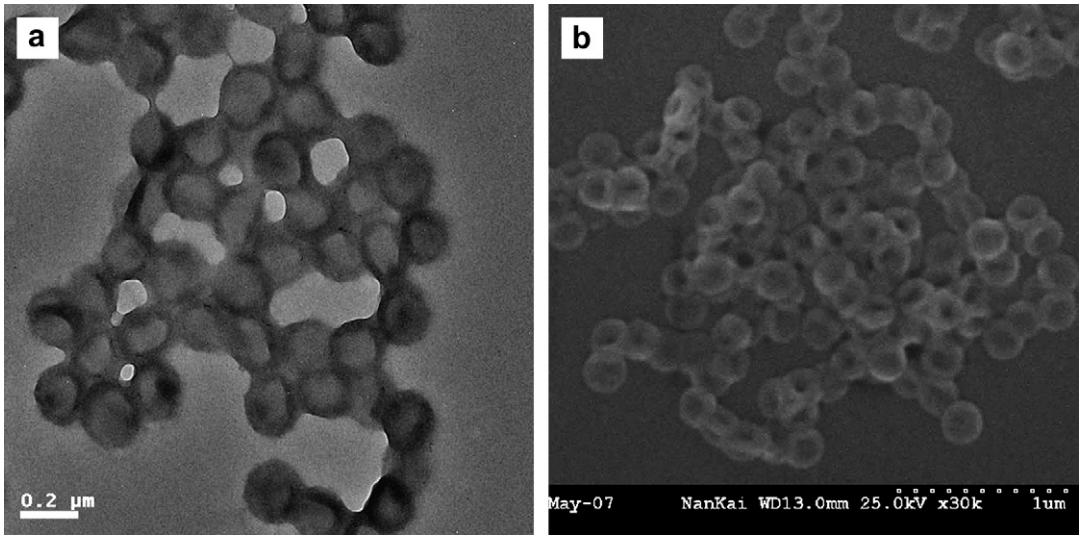

Fig. 4. PNIPAAm hollow microspheres of $H_{20\text{-}2}$: (a) TEM; (b) SEM.

Table 3
Characteristics of temperature-responsive PNIPAAm hollow microspheres

Entry	Crosslinking degree (mol%)	NIPAM/PMAA (w/w)	D_h[a] (nm)	U[a]
H_{10-1}	10	1	315	1.136
H_{10-2}	10	2	330	1.165
H_{10-3}	10	3	470	1.238
H_{10-4}	10	4	483	1.198
H_{5-2}	5	2	283	1.257
H_{15-2}	15	2	331	1.198
H_{20-2}	20	2	294	1.196

[a] Hydrodynamic diameters from DLS determined at scattering angle of 90°.

hydrodynamic diameters and their distribution with various NIPAAm feeds for the second-stage polymerization are illustrated in Fig. 5a. All the hydrodynamic sizes of the hollow microspheres were a little larger than those of the corresponding diameters of the core–shell microspheres from TEM characterization, which indicated that the PNIPAAm hollow microspheres were under a swollen state in water due to the hydrophilic nature of the hollow microspheres. The hydrodynamic diameters of the hollow microspheres with high crosslinking degree changed less significantly than the ones with low crosslinking degree. Such results indicated

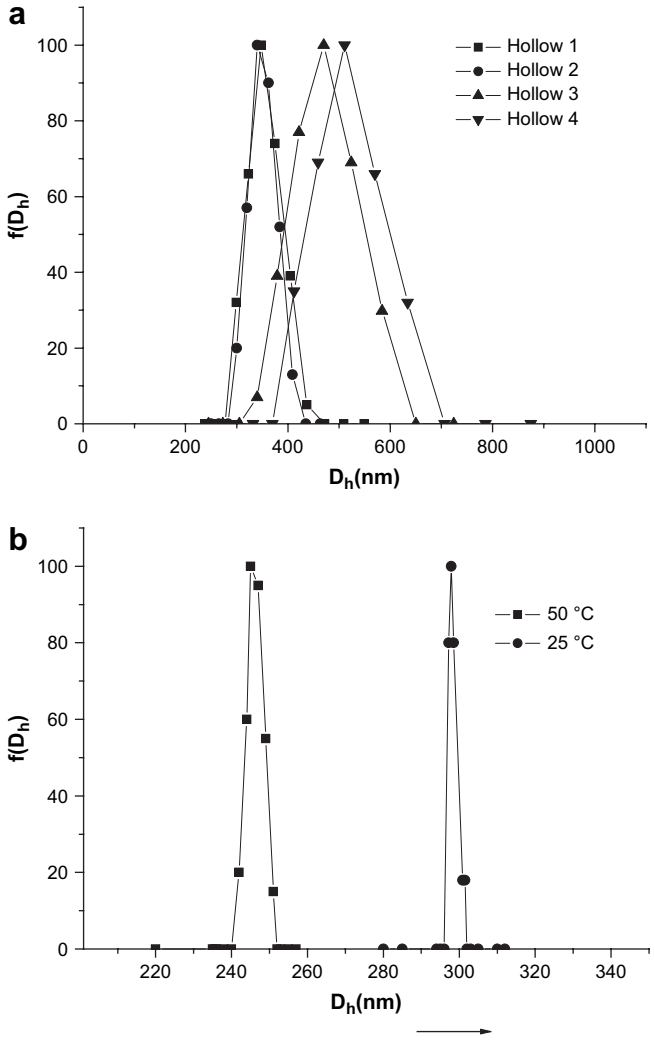

Fig. 5. Hydrodynamic diameters and their distribution: (a) hollow PNIPAAm microspheres with different shell thicknesses and crosslinking degrees; (b) hollow PNIPAAm microspheres under different environmental temperatures with H_{20-2} as a sample.

Table 4
DLS and SLS results of PNIPAAm hollow microspheres

Entry	T (°C)	D_h[a] (nm)	R_g[b] (nm)	R_g/R_h	U
H_{20-2}	25	294	206	1.50	1.196
	50	265	207	1.56	1.154

[a] Value from DLS determined at scattering angle of 90°.
[b] SLS measurement performed from 50° to 125°.

that the PNIPAAm hollow microspheres with higher MBAAm crosslinking degree were in a less swollen state.

The temperature–stimuli volume transition of the PNIPAAm hollow microspheres was recorded by DLS measurement of H_{20-2}. The hydrodynamic diameter (D_h) of the hollow PNIPAAm microspheres decreased considerably from 294 to 265 nm when the environmental temperature was increased from 25 to 50 °C as illustrated in Fig. 5b. According to the DLS results, the swelling ratio under different temperatures defined as $(D_{25}/D_{50})^3$ was calculated as 1.36, which confirmed the thermo-responsive characteristic of the resultant PNIPAAm hollow microspheres, even in the case of the highest degree of 20 mol% MBAAm in the present work. A combination of DLS and SLS measurements affording the ratio of average gyration radius to the corresponding average hydrodynamic radius (R_g/R_h) is listed in Table 4. It is well known that the R_g/R_h values reflect the morphology or conformation of the chains or the density distribution of the particles in the solution [36,37]. The R_g/R_h values of the PNIPAAm hollow microspheres (H_{20-2}) were maintained at around 1.50 under both 25 and 50 °C, which was significantly higher than the typical value of 0.774 for the uniform microspheres. This result demonstrated that the resultant PNIPAAm particles had a hollow structure, which was in accordance with the results from TEM and SEM observations.

3.3. Loading and releasing behavior of DXR on PNIPAAm hollow microspheres

To evaluate the potential application of PNIPAAm microspheres as a drug carrier, DXR was used as the model to carry out the loading and releasing test, in which the hollow microspheres of H_{15-2} was used as the sample. The kinetics of DXR incorporated onto the PNIPAAm hollow microspheres were analyzed by the residual DXR remaining in the solution during the loading process, in which the loading amount of DXR onto the hollow polymer microspheres is illustrated in Fig. 6a. At the initial stage, the amount of the DXR loaded onto the PNIPAAm hollow microspheres was increased quickly with the loading time and then leveled off after 20 h. The final loading capacity of DXR onto the PNIPAAm hollow microspheres was about 15.8 μg/mg.

The controlled drug releasing behavior of DXR loaded onto PNIPAAm hollow microspheres was investigated. The DXR loaded onto hollow microspheres was released steadily and slowly, which may perform the accumulation of DXR in the heart muscle. Fig. 6b shows the kinetics of DXR releasing from hollow PNIPAAm microspheres under different environmental temperatures, which indicated that the DXR release behavior depended on the temperature of the solution. The half times of the releasing were 32 h at 20 °C and 54 h at 40 °C. For the DXR released from the PNIPAAm hollow microsphere at 40 °C, the DXR could be released more slowly, which may be originated from the temperature-dependent swelling transition property of the hollow microspheres involving the PNIPAAm segments with a well-known phase transition temperature at around 32 °C. During such transition, the gate pores for the drug release were in a shrinking state at 40 °C and a swelling state at 20 °C on the shell layer of the PNIPAAm hollow carrier, which enabled the hollow microspheres to have a tunable-controlling release property for the loaded drugs between the interior of hollow microspheres and the bulk medium under different

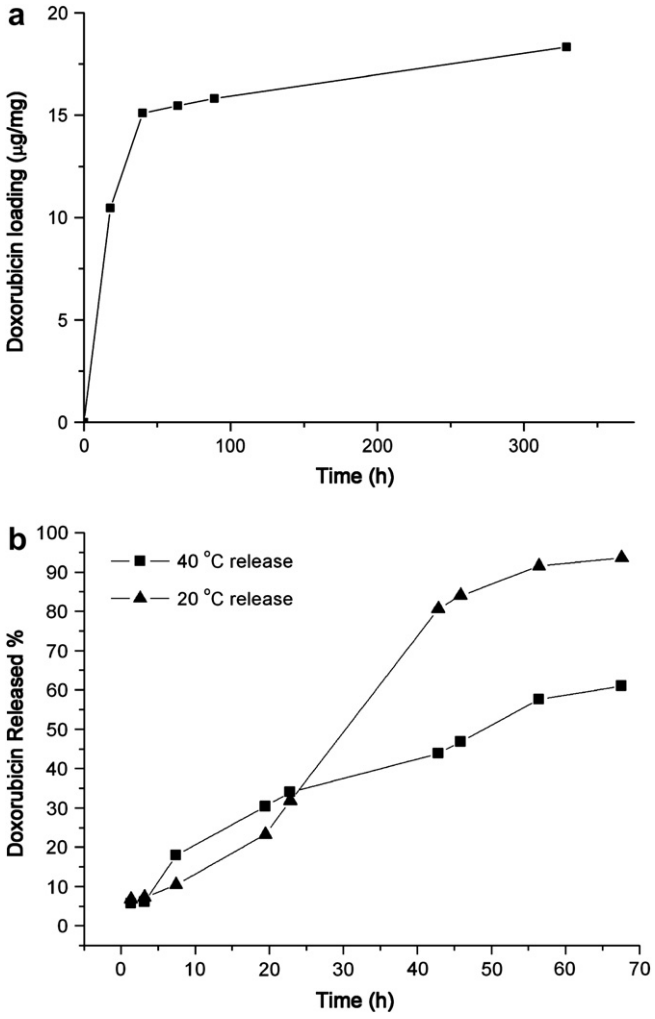

Fig. 6. Loading and controlled releasing of DXR on PNIPAAm hollow microspheres ($H_{20\text{-}2}$): (a) the relationship between the loading amount of DXR and the loading time; (b) controlled release of DXR from PNIPAAm hollow microspheres under different temperatures.

environmental temperatures. The ability for the release of DXR above LCST of PNIPAAm (40 °C) may be due to the presence of porous structure in the PNIPAAm shell of the hollow polymer microspheres, especially the hollow microspheres under a swollen state in water with hydrophilic MBAAm as crosslinker. The porous structure of poly(divinylbenzene-*co*-acrylic acid) (poly(DVB-*co*-AA)) shell was observed clearly by a TEM micrograph with higher magnification for poly(DVB-*co*-AA) hollow microspheres with movable poly(DVB-*co*-AA) cores [38]. These tiny pores permitted the PMAA with molecular weight as high as 1.44×10^4 to diffuse out of the highly crosslinked shell during the selective removal of non-crosslinked core for the formation of the hollow functional polymer microspheres. The drug loading and releasing behavior of the hollow PNIPAAm microspheres controlled by the different environmental temperatures, thickness of the shell layer and the crosslinking degree is now being studied in detail by our group.

4. Conclusion

Hollow PNIPAAm microspheres with different shell thicknesses and degree of crosslinkings were prepared by a facile route with a two-stage distillation precipitation polymerization in neat acetonitrile with AIBN as initiator and subsequent removal of PMAA core by dissolution in water. The formation of monodisperse PMAA@PNIPAAm core–shell microsphere was driven by the synergic hydrogen-bonding interaction between the carboxylic acid group on the surface of PMAA seeds and the amide group of MBAAm as well as NIPAAm unit during the second-stage polymerization of MBAAm crosslinker and NIPAAm, in which the feed of monomer and the MBAAm crosslinking degree had much effect on the morphology and the shell thickness of the core–shell microspheres. The PNIPAAm hollow microspheres were then developed by the selective removal of PMAA cores from the core–shell microspheres, which was confirmed further by the results from TEM, elemental analysis, DLS and SLS characterization. The primary results about the controlled release of DXR from the PNIPAAm hollow microspheres indicated that the extent of release could be tuned by the environmental temperature originating from the various permeability of the shell layer due to the presence of thermo-responsive PNIPAAm segments.

Acknowledgement

This work was supported by the National Science Foundation of China (Project No. 20504015).

References

[1] Wooley KL. J Polym Sci Part A Polym Chem 2000;38:1397.
[2] Li ZC, Jin W, Li FM. React Funct Polym 1999;42:21.
[3] Schirrer R, Lanke R, Boudouaz J. Polym Eng Sci 1997;37:1748.
[4] Pathak S, Greci MT, Kwong RC, Mercado K, Prokash SGK, Olah GA, et al. Chem Mater 2000;12:1985.
[5] Tamber H, Johansen P, Merkle HP, Gander B. Adv Drug Delivery Rev 2005;57:357.
[6] Sinha VR, Trehan A. J Controlled Release 2003;90:261.
[7] Hammer DA, Discher DE. Annu Rev Mater Sci 2001;31:387.
[8] Raymond MC, Neufeld RJ, Poncelet D. Artif Cells Blood Substitutes, Immobilization Biotechnol 2004;32:275.
[9] Zhang J, Xu S, Kumacheva E. J Am Chem Soc 2004;126:7908.
[10] McDonald CJ, Bouck KJ, Chaput AB, Stevens CJ. Macromolecules 2000;33:1593.
[11] Xu XL, Asher SA. J Am Chem Soc 2004;126:7940.
[12] Pavlyuchenko VN, Sorochinskaya OV, Ivanchev SS, Klubin VV, Kreichman GS, Budtov VP, et al. J Polym Sci Part A Polym Chem 2001;39:1435.
[13] Zha LS, Zhang Y, Yang WL, Fu SK. Adv Mater 2002;14:1090.
[14] Mandal TK, Fleming MS, Walt DR. Chem Mater 2000;12:3481.
[15] Glinel K, Sukhorukov GB, Möhwald H, Khrenov V, Tauer K. Macromol Chem Phys 2003;204:1784.
[16] Donath E, Sukhorukov GB, Caruso F, Davis SA, Möhwald H. Angew Chem Int Ed 1998;37:2201.
[17] Park MK, Onishi K, Locklin J, Caruso F, Advincula RC. Langmuir 2003;19:8550.
[18] Stewart S, Liu GJ. Chem Mater 1999;11:1048.
[19] Fu GD, Shang Z, Hong L, Kang ET, Neoh KG. Macromolecules 2005;38:7867.
[20] Sauer M, Streich D, Meier W. Adv Mater 2001;13:1649.
[21] Ibarz G, Dahen L, Donath E, Möhwald H. Adv Mater 2001;13:1324.
[22] Shiga K, Muramatsu T, Kondo T. J Pharm Pharmacol 1996;48:891.
[23] Brown MD, Schatzlein A, Brownlie A, Jack V, Wang W, Tetley L, et al. Bioconjugate Chem 2000;11:880.
[24] Son YJ, Jang JS, Cho YW, Chung H, Park RW, Kwon IC, et al. J Controlled Release 2003;91:135.
[25] Kabanov AV, Batrakova EV, Alakhov VY. J Controlled Release 2003;91:75.
[26] Sadzuka Y, Nakade A, Tsuruda T, Sonobe T. J Controlled Release 2003;91:271.
[27] Mayer LD, Cullis DR, Bally MB. J Liposome Res 1994;4:529.
[28] Bai F, Yang XL, Huang WQ. Macromolecules 2004;37:9746.
[29] Bai F, Huang B, Yang XL, Huang WQ. Polymer 2007;48:3641.
[30] Bai F, Yang XL, Li R, Huang B, Huang WQ. Polymer 2006;47:5775.
[31] Liu GY, Yang XL, Wang YM. Polymer 2007;48:4385.
[32] Li GL, Yang XL, Bai F. Polymer 2007;48:3074.
[33] Bai F, Huang B, Yang XL, Huang WQ. Eur Polym J 2007;43:3923.
[34] Li R, Yang XL, Li GL, Li SN, Huang WQ. Langmuir 2006;22:8127.
[35] Liu GY, Zhang H, Yang XL, Wang YM. Polymer 2007;48:5896.
[36] Wan X, Tu Y, Zhang D, Zhou Q, Wu C. J Am Chem Soc 2000;122:10201.
[37] Wu C, Zuo J, Chu B. Macromolecules 1989;22:633.
[38] Li GL, Yang XL. J Phys Chem B 2007;111:12781.